Polymerization of acrylamide in a swollen lamellar mesophase

C. Holtzscherer*, J. C. Wittmann, D. Guillon and F. Candau†
Institut Charles Sadron (CRM-EAHP), CNRS, 6 rue Boussingault, 67083 Strasbourg Cédex, France
(Received 20 October 1989; accepted 16 November 1989)

Polymerization of acrylamide in a liquid-crystalline phase swollen by large amounts of oil and water and showing long-range smectic order has been investigated. The macroscopic properties of the systems during polymerization were followed by viscometry, turbidimetry and ^1H nuclear magnetic resonance experiments. The microscopic structures were analysed by small-angle X-ray diffraction and optical microscopy. Polymerization of acrylamide transformed the initial lamellar phase to an isotropic, clear and stable microlatex formed of water-swollen polymer particles dispersed in the oil. This result was accounted for by the monomer acting as co-surfactant at the interface and the large-scale undulations of the flexible lamellae.

(Keywords: lamellar phase; polymerization of acrylamide in a lamellar phase; microlatex; polyacrylamide; small-angle X-ray scattering of a polymerizable lamellar phase)

INTRODUCTION

Liquid crystals provide attractive media for specific reactions such as polymerization. The polymerization reaction can be achieved in two ways. One consists of polymerizing a mesomorphic monomer, leading to a product with a 'locked-in' mesomorphic structure. These systems have the great advantage of consisting of a single component; they have been the subject of numerous studies[1–6]. The second possibility is to polymerize a monomer inserted in a lyotropic liquid-crystalline structure. The complexity of these multicomponent systems explains the paucity of papers in the literature. The attempts have usually met with limited success; the initial mesomorphic structure was not retained[6–8] or a rearrangement of the microstructure occurred through polymerization[9]. The conformational loss of entropy during polymerization, as well as incompatibility between the matrix and polymer, were the factors usually invoked to explain the results.

In previous work, we reported on a study of the polymerization of acrylamide in non-ionic microemulsions[10–12]. The latter are disordered and thermodynamically stable dispersions of oil and water stabilized by the addition of suitable surfactants[13]. Their optical transparency is a consequence of the small size of the oil (or water) regions. The non-ionic microemulsions used in our study were formulated with the help of the cohesive energy ratio (*CER*) concept[11]. It was shown that additives such as electrolytes induced the formation of bicontinuous microemulsions[12]. In this case, the microemulsions were not closed structures (such as water or oil droplets dispersed in oil or water, respectively) but had the oil and water regions connected over macroscopic distances and separated by a surfactant monolayer film. These isotropic bicontinuous microemulsions were characterized by very low interfacial tensions ($\simeq 10^{-3}$ dyn cm^{-1}) and they led after polymerization to very stable and clear microlatices of polyacrylamide particles dispersed in oil. Liquid-crystalline phases showing long-range smectic order and containing higher surfactant concentrations ($\simeq 22\%$) were also observed in the phase diagram close to the microemulsion domains. Surprisingly, polymerization of acrylamide in these lamellar microemulsions gave very stable microlatices similar to those prepared in bicontinuous microemulsions.

In order to gain further insight into the polymerization mechanism occurring in these structures, we have followed their development during polymerization. For this purpose, we have used methods providing information on the macroscopic properties of the systems: viscometry, turbidimetry, polymerization yield and compositions of the phases at equilibrium. In addition, small-angle X-ray diffraction and optical microscopy allowed us to characterize their microscopic structures.

The first step of the polymerization process was accompanied by phase separation. We have undertaken two types of experiments. In the first, the system was polymerized under stirring; in the second, it was polymerized without stirring. After having characterized the microscopic structure of the starting system, we analysed successively the evolution of the polymerization for each of the experimental conditions described above.

EXPERIMENTAL

Materials

Acrylamide (AM) from Fluka was recrystallized twice from chloroform. Water was double-distilled. The oil is a narrow-cut isoparaffinic mixture, Isopar M from Esso Chemie, which was filtered before use (boiling range 207–257°C). The surfactant blend (Arlacel 83 plus G

* Present address: Faculté de Pharmacie, Laboratoire de Pharmacie Galénique, CNRS URA D 1218, 5 Rue J. Baptiste Clément, 92296 Chatenay-Malabry Cédex, France
† To whom correspondence should be addressed

0032-3861/90/101978-08

1086) was supplied by Atlas Chemical Industries NV and was used without further purification. Azobisisobutyronitrile (AIBN; Merck) was used as the initiator of the polymerization and was recrystallized twice from ethanol and stored in dark bottles in a refrigerator. Microemulsions were prepared (wt/wt) by adding the aqueous solution of acrylamide to the mixture of emulsifiers, AIBN and Isopar M.

Polymerization procedure

The polymerization reactions were run at 20°C according to two different procedures. A series of experiments were performed under stirring in a water-jacketed reaction vessel after bubbling nitrogen through the microemulsion to eliminate oxygen. The acrylamide was initiated with AIBN (0.3% based on monomer) under u.v. irradiation (mercury lamp, Philips). The reaction vessel is shown in *Figure 1*.

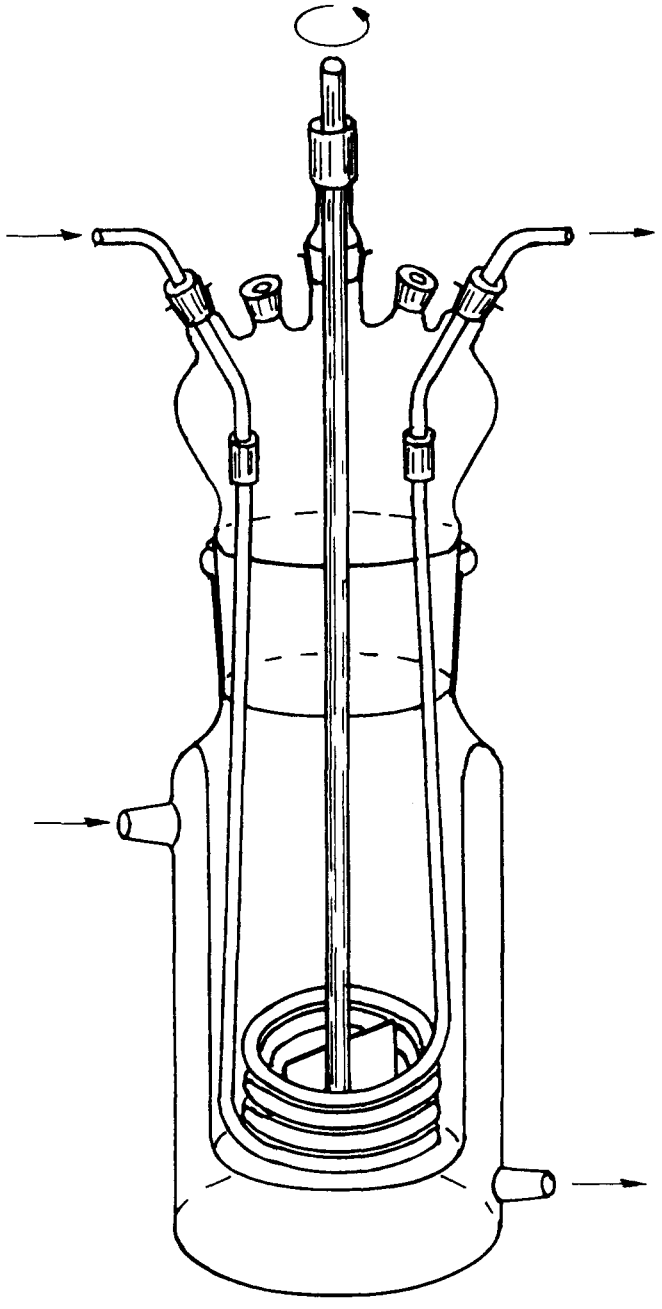

Figure 1 Schematic representation of the apparatus used for the polymerization of acrylamide

An additional inner thermostat formed by a stainless-steel coil immersed in the solution ensured good removal of the heat developed during the polymerization of acrylamide. Efficient stirring was achieved by means of an electrically driven blade stirrer. The reaction vessel lid has five entries: two for the cooling coil, one for the stirrer and the two others were used as needed for nitrogen bubbling, sampling or temperature probe.

Samples of the latex were taken from the polymerization cell by syringe at various stages of the polymerization, and the reaction was stopped by adding hydroquinone monomethyl ether as inhibitor (<100 ppm). Half of the sample solutions were used for turbidimetry, viscometry, X-ray diffraction and optical microscopy. The rest of the samples were used to recover the polymer by precipitation in a large excess of acetone, followed by several washings, filtration and drying under vacuum at 45°C. The percentage conversion was determined by gravimetry and the molecular weight of the polymer by viscometry (see below).

The second polymerization procedure that we used was to follow the progress of polymerization of a series of systems of the same compositon, placed in sealed test tubes and exposed to daylight in the absence of stirring. The polymerization was spontaneously initiated within the first 30 min and was completed within 24 h. The experiments were repeated several times in order to check the reproducibility of the results. Structural changes of the lamellar phase were followed by small-angle X-ray diffraction. The evolution in the system composition was analysed by ^{1}H n.m.r.

^{1}H n.m.r. spectra

N.m.r. spectra were run on a 60 MHz Bruker AW 80 spectrometer at 25°C. The chemical shifts were expressed in δ units using hexamethyldisilane (HMDS) as the external reference.

Turbidimetry

The optimal transmittance of the systems was measured spectrophotometrically at 25°C, using a helium–neon laser as a monochromatic source of light. The transmittance is expressed as (percentage) transmission coefficient $T = I/I_0$, where I_0 is the intensity of the incident light and I the intensity of the light transmitted through the cell.

Small-angle X-ray diffraction

X-ray diffraction[14] data were collected using a vacuum small-angle camera[15] equipped with a bent gold-plated glass mirror (Ni-filtered Cu Kα radiation from a GX20 Eliott rotating-anode X-ray generator). The patterns were registered photographically, the time exposure being 30 min. Samples were contained in 1.5 mm thick Lindemann capillaries.

Viscometry

The viscosities of the concentrated systems were measured at 25°C with a Couette viscometer (Rheomat 30 Contraves). This apparatus allows one to measure viscosities of Newtonian and non-Newtonian solutions over a wide range of shear rates (6.24 to 1800 s^{-1}).

Polymers have been characterized by their intrinsic viscosities in 0.1 M NaCl aqueous solutions measured at 25°C with an automatic capillary viscometer. All

measurements were performed with the same capillary of 0.46 mm diameter. The viscosity becomes non-Newtonian, even at the lowest shear rate attainable in our experiments, at intrinsic viscosities higher than 430 $cm^3 g^{-1}$. In such cases, we have used the empirical law determined at finite gradient by François *et al.*[16]. For lower values of the viscosity, we have used the following relationship proposed by the same authors:

$$[\eta] = 9.33 \times 10^{-3} M_w^{0.75} \text{ cm}^3 \text{ g}^{-1}$$

Optical microscopy

Microstructures were observed with a Zeiss Photomicroscope II equipped with crossed nicols and phase contrast. Both techniques were used to characterize and follow:

(a) in polarized light, the disappearance with time of the initial birefringent liquid-crystalline phase and,

(b) under phase contrast, the concomitant phase separation and formation of an isotropic phase.

RESULTS

The system prior to polymerization

The system that was investigated has the following composition (wt/wt): Isopar M, 41.5%; surfactant blend (hydrophile–lipophile balance, $HLB = 9.3$), 22.1%; acrylamide, 14.2%; water, 20.1%; sodium acetate (NaAc), 2.1%. The volume fraction of the disperse phase is 51.5%. The system has a low viscosity ($\eta \simeq 160$ mPa) and a pseudoplastic behaviour; its optical transmittance is 94%. Optical microscopic observations between crossed polarizers show oily streaks, which are characteristic of a lamellar liquid-crystalline phase (*Figure 2a*). Under phase contrast, the system appears perfectly homogeneous. The X-ray diffraction pattern gives a single sharp line corresponding to an interlayer spacing $s^{-1} = 197$ Å. The absence of higher-order diffraction lines can be accounted for by the internal dynamics of the system associated with the high dilution of these four-component systems, as discussed by several authors[17–23].

Other measurements performed on various microemulsions of the same composition gave a periodicity of the lamellar phase ranging between 196.6 and 199.7 Å, which confirmed the excellent reproducibility in the preparation of the sample.

Since the interlayer spacing ($s^{-1} \simeq 197$ Å) is much higher than the average length of the fully extended surfactant molecules (51 Å for G 1086 and 32 Å for Arlacel 83), it can be inferred that the microscopic structure of the system corresponds to highly swollen layers of oil and water. This result corroborates previous studies, which reported that some microemulsions can be formed of hyperswollen lamellar phases whose periodicity can reach 1000 Å or more[17–22].

The thickness of the sheets swollen by water and oil (s_w^{-1} and s_0^{-1} respectively) can be calculated from the following relationships:

$$s^{-1} = s_0^{-1} + s_w^{-1}$$

$$s_0^{-1} = s^{-1}\left(1 + \frac{V_w}{V_o}\right)^{-1}$$

with

$$V_o = x_{\text{Isopar}} v_{\text{Isopar}} + x_L v_L$$

$$V_w = x_{H_2O} v_{H_2O} + x_{AM} v_{AM} + x_{NaAc} v_{NaAc} + x_H v_H$$

The parameters x_i and v_i represent respectively the weight fraction and the specific volume of component i; the subscripts H and L refer respectively to the hydrophilic moiety and lipophilic tail of the surfactants. A schematic structure of the lamellar phase is given in *Figure 3*.

The ^{1}H n.m.r. spectrum of the microemulsion is rather complex (*Figure 4*). The series of peaks observed at chemical shifts δ ranging between 5.5 and 7.7 ppm correspond to acrylamide; the signal at 1.8 ppm, which is attributed to sodium acetate, partially overlaps that of Isopar M. The peak centred at $\delta = 3.5$ ppm is associated with the methylene groups of the surfactants.

Polymerization of acrylamide

Under stirring. The polymerization procedure has been described in the 'Experimental' section. Because of the speed of the reaction, it was not possible to perform all the measurements in a single experiment. The data reported in *Figure 5* were therefore obtained from separate experiments, which were replicated in order to confirm their reproducibility. The variation of the percentage conversion p *versus* time (*Figure 5a*) shows that the polymerization proceeds in two steps. In the initial stage of the reaction, the conversion increases slowly with time, up to about 20% conversion ($t = 5$ min). Beyond this point, one observes a sudden increase in the slope of the curve, which reflects an acceleration of the polymerization reaction. A quantitative yield is obtained at $t = 8$ min.

The molecular weight of the polymer is almost independent of the degree of conversion ($\simeq 5.3 \times 10^6$), as expected for a free-radical polymerization mechanism (*Figure 5c*).

In parallel with the above measurements, we have analysed for each sample the changes produced by the formation of polymer by viscosity and turbidity measurements. *Figures 5a* and *5b* present respectively the variations with time of the optical transmittance and of the viscosity of the system. As soon as the polymerization starts, one observes a dramatic decrease of the transmittance accompanied by a strong increase of the absolute viscosity; these are directly related to the formation of a two-phase system.

The transmittance remains near zero from $t = 2.5$ min ($p \simeq 5\%$) to $t = 5.5$ min ($p \simeq 50\%$). During this time, the viscosity of the medium increases to values larger than 1500 mPA and cannot be accurately measured. Beyond $t = 5$ min, latex formation is evidenced by the transparency of the system and by a sharp drop of the viscosity, which reaches 50 mPA at the end of the reaction ($t = 8$ min, $p = 100\%$).

The two-step polymerization process can be explained by the combined effects of viscosity and transmittance. When the system becomes turbid and two-phase in the early stages of the polymerization, the resulting decrease in u.v. transmittance and the increased viscosity combine to slow down the rate of polymerization. In the second step, the transparency of the system together with the low viscosity, which ensures a good homogenization, produce the observed enhancement of the reaction rate.

A more direct indication of the microstructure of the system and its evolution with time was provided by microscopy under phase contrast and polarized light. This is illustrated by the sequence of photomicrographs (b) to (j) reported in *Figure 2*. In the early stage of the

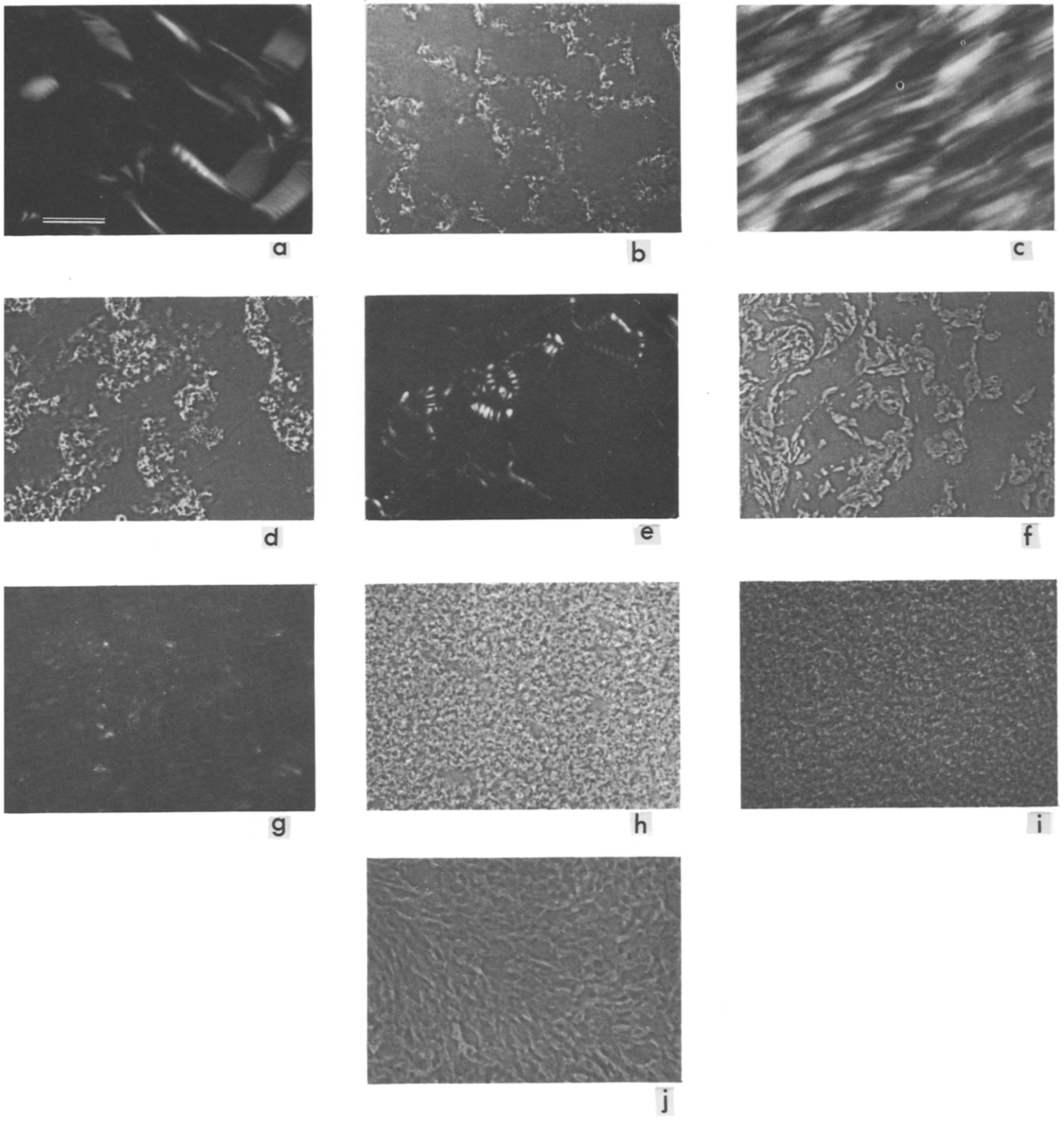

Figure 2 Sequence of polarized-light and phase-contrast optical photomicrographs showing the evolution with u.v. irradiation time t of the polymerizing system (scale bar, 50 μm): (a) $t=0$, starting fluid lamellar phase as revealed by the presence of oily streaks; (b)–(e) $t=1$ min, disruption of the lamellar phase along with the formation of an isotropic phase ((d) and (e) same area); (f) $t=1$ min 50 s; (g), (h) $t=5$ min 30 s; (i) $t=5$ min 50 s; (j) $t=6$ min 30 s, ultimate stage before complete isotropy

reaction, the diminution of the transmittance corresponds to the appearance in phase contrast of bright, fragmented structures dispersed in a homogeneous continuous medium (*Figure 2b*). Under polarized light, one observes a fluid birefringent phase, which takes on within a few minutes a homeotropic configuration with a few residual oily streaks (*Figure 2c*). A comparison of the same area in phase contrast (*Figure 2d*) and in polarized light (*Figure 2e*) allows one to identify the two coexisting phases. The residual oily streaks appear under phase contrast in the continuous medium and at the border of the fragmented domains. The homogeneous continuous phase thus corresponds to the fluid birefringent lamellar phase, whereas the fragmented domains are isotropic.

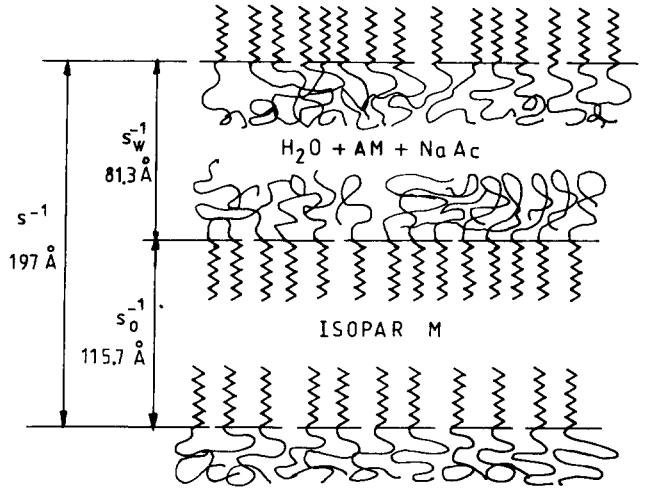

Figure 3 Schematic model of the lamellar phase

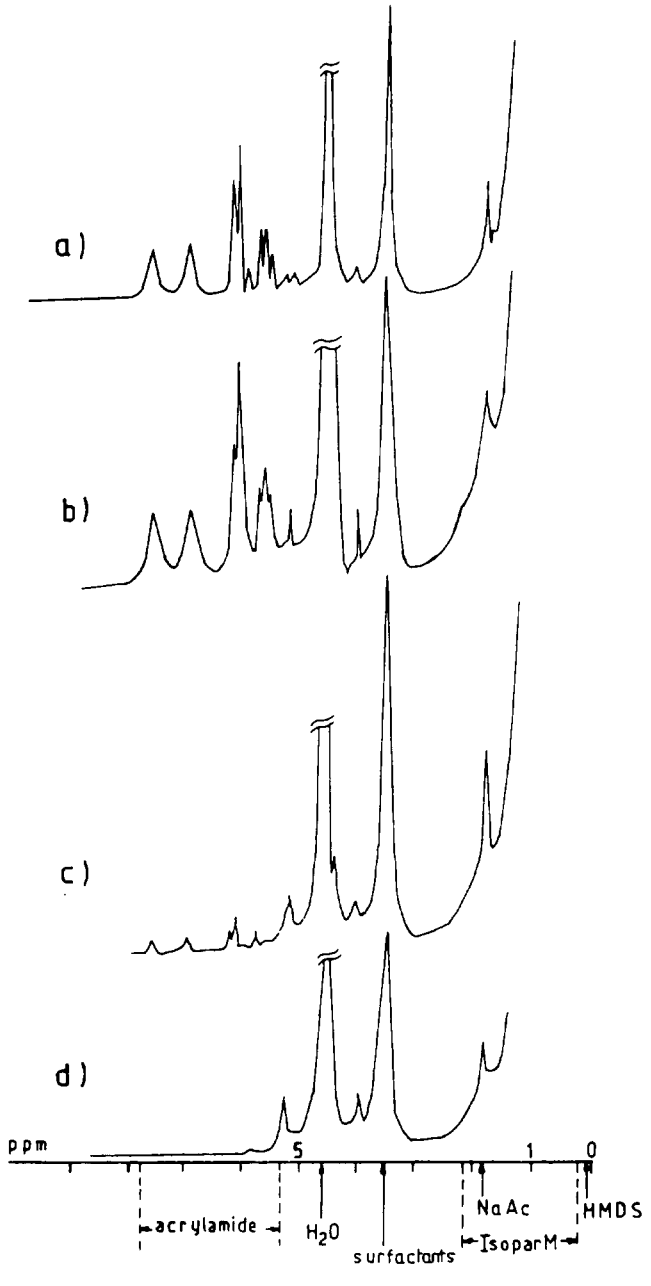

Figure 4 ^1H n.m.r. spectra: (a) initial system; (b), (c) polymerization in the absence of stirring, end of the second step ((b) upper phase, (c) lower phase); (d) final system

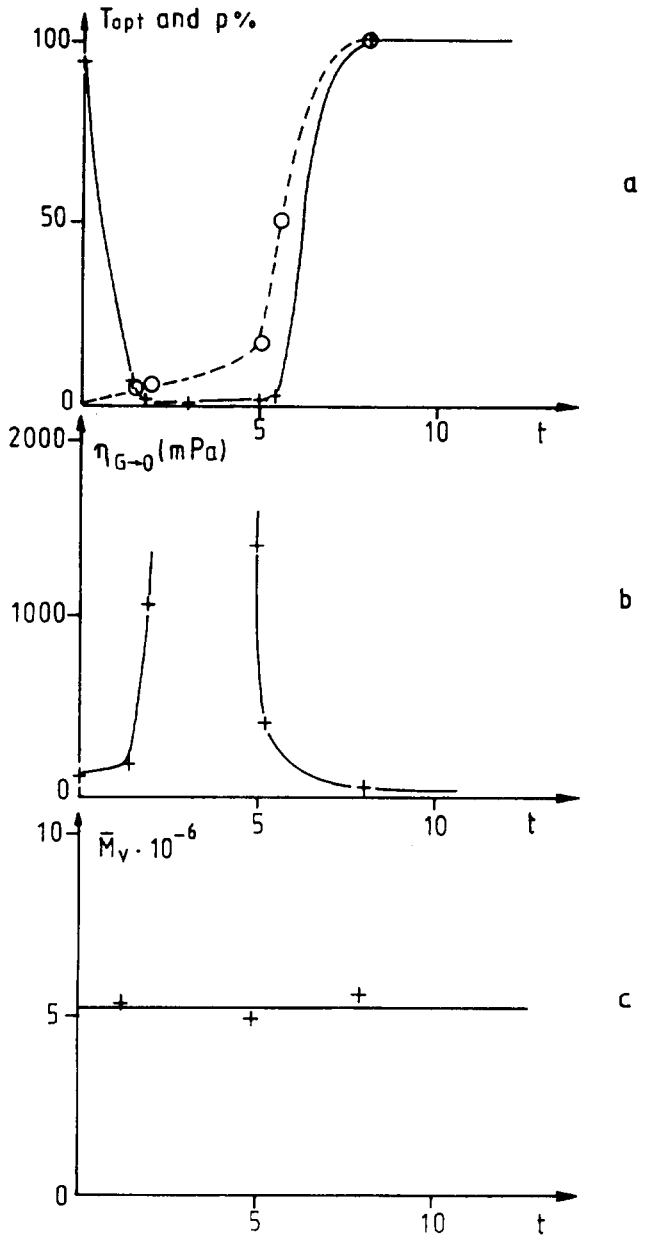

Figure 5 Development of the polymerization of acrylamide in a lamellar phase with u.v. irradiation time t (min): (a) optical transmittance T_{opt} (+) and percentage of conversion (○); (b) viscosity at zero shear rate, $\eta_{G\to0}$; (c) molecular weight of polyacrylamide, $\bar{M}_v$

When the reaction proceeds, the space available for the lamellar phase shrinks in favour of the isotropic phase (*Figure 2f*). Micrographs (g) and (h) correspond to $t = 5$ min 30 s when 50% of AM has polymerized. The system has lost most of its birefringent character, reflecting the disappearance of the lamellar phase. In phase contrast, it can be seen that the isotropic domains cover the major part of the area and become more and more fragmented (*Figure 2i*). At the end of the reaction, the fragmented domains coalesce (*Figure 2j*) and finally disappear, giving rise to a perfectly fluid isotropic phase.

In the absence of stirring. The system to be polymerized was divided in equal proportions into different tubes, which were left on the shelf and exposed to daylight. Macroscopic observations of the polymerization process led us to distinguish three steps, which were analysed by

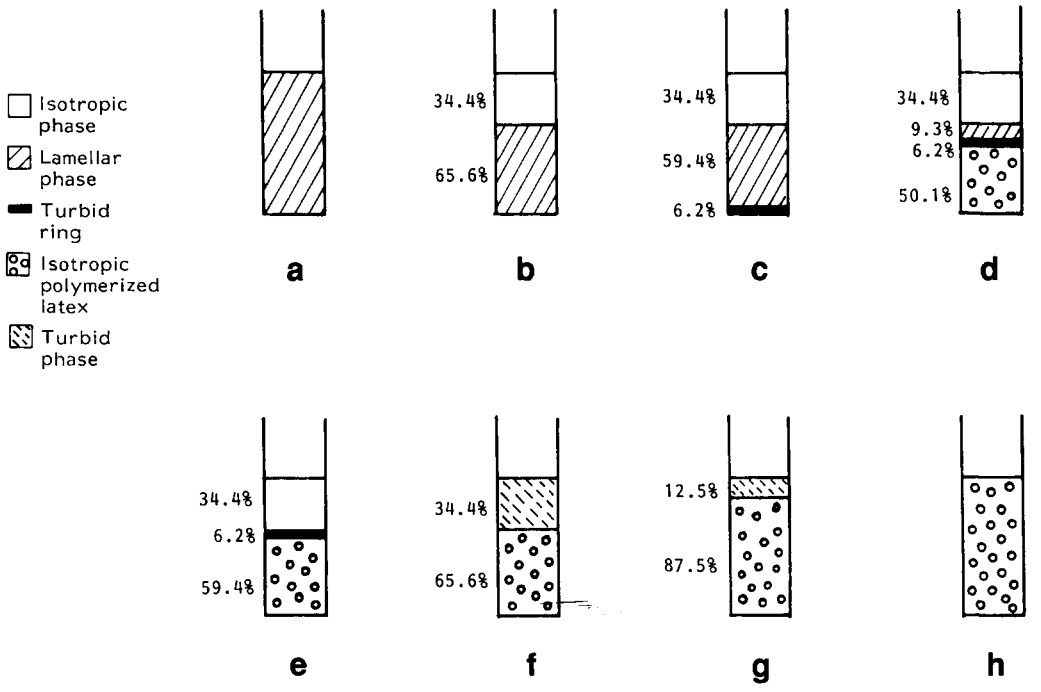

Figure 6 Schematic drawings showing the evolution of the system during the polymerization of acrylamide in the absence of stirring: (a) initial lamellar system ($s^{-1} = 197$ Å); (b) phase separation; (c)–(e) polymerization of the lower phase; (f), (g) polymerization of the upper phase; (h) final latex

the following techniques:

(i) optical microscopy and low-angle X-ray diffraction for the birefringent phases;

(ii) qualitative ^{1}H n.m.r. analysis of the different phases that coexist during the reaction;

(iii) detection of polymer formation by precipitation of the system in acetone.

The data resulting from these observations are shown by the schematic drawings of *Figure 6*. Examination of these drawings suggests the following process for this polymerization reaction.

The first step corresponds to the start of the polymerization; the lamellar system ($s^{-1} = 197$ Å) separates into two clear phases, an isotropic phase and a lamellar phase characterized by a periodicity of 188 Å. Both phases contain all of the components. This step is achieved within 2 h (drawings (a) and (b)).

The second step, illustrated by drawings (c)–(e), corresponds to the polymerization of AM occurring predominantly at the bottom of the tube (turbid ring). Under the microscope, the turbid ring, which has the consistency of a membrane, shows fragmented structures very similar to those observed under stirring (*Figure 2f*). These structures could refer to the hydrated polyacrylamide clusters. As the polymerization proceeds, the ring rises in the tube and divides the previous lamellar phase into two parts. Under the ring is a fluid polymer phase. ^{1}H n.m.r. spectral analysis shows the presence of all the components except acrylamide, indicating that this phase has a structure similar to that of the final latex, i.e. water-swollen polymer particles dispersed in Isopar M. Above the ring is the lamellar phase in contact with the upper isotropic phase. Both phases contain acrylamide but no polymer as shown by the negative results of ^{1}H n.m.r. spectroscopy and precipitation tests. A simultaneous decrease of volume and periodicity of the lamellar phase with time is observed ($s^{-1} = 158$ Å, drawing (d)).

At the end of the second step, the lamellar phase has completely disappeared and the turbid ring delimits two isotropic phases (drawing (e), *Figures 4b* and *4c*). It should be noted that all of the polymer formed is concentrated into the lower phase and in the ring (59.4% and 6.2% respectively). This result is in good agreement with a control experiment in which we checked that the density of the latex ($d \simeq 0.94$) was higher than that of the initial microemulsion ($d \simeq 0.91$).

In the third step (*Figure 6*, drawings (f) and (g)) the polymerization proceeds in the upper phase, which becomes turbid. When the yield of the reaction is quantitative, one gets a clear ($T_{opt} \simeq 98\%$) fluid and single-phase latex (drawing (h), *Figure 4d*), which appears perfectly homogeneous in phase contrast.

An analysis of the final latex gives characteristics similar to those previously observed for latices prepared in microemulsions, i.e. a concentrated dispersion of spherical particles as shown by electron microscopy (EM) and quasi-elastic light scattering (QELS)[10,24]. The latex shows a Newtonian behaviour with a viscosity of 50 mPa. QELS experiments gave a diameter of 74 nm with a variance of the autocorrelation function of the scattered intensity of 0.03. The latter result is indicative of a rather low polydispersity of the system[10].

DISCUSSION

The results give clear evidence of a polymerization-induced structural change from an initial swollen lamellar phase to a final homogeneous dispersion of spherical particles. The polymerization of acrylamide immediately promotes phase separation and transfer of monomer from the organized mesophase to a disordered isotropic phase. Similar behaviour has been encountered in the polymerization of monomers inserted in ternary lyotropic mesophases, and was first described for the polymerization of lipophilic monomers in a water–soap lamellar

phase[6]. Phase separations or structural modifications were also mentioned in polymerization studies involving other types of lyotropic liquid-crystalline phases[7–9]. A specific feature of the system investigated here is that the final state is a single phase, namely an isotropic, clear and stable latex, whereas in some other studies, phase separation was observed throughout the reaction[6].

The above results can be contrasted with polymerization experiments carried out in binary mixtures of soap and water or in one-component systems where the amphiphile acts also as the monomer. In these cases, the organization of the lamellar phase could be successfully 'locked in' through polymerization[1–6]. Special mention should also be made of recent polymerization experiments in which the microstructure of a lyotropic bicontinuous cubic phase was preserved[25]. In contrast with birefringent microemulsions, bicontinuous cubic phases are extremely viscous; the very slow rate of rearrangement of the periodic microstructure may account for this result.

Several factors are responsible for the structural change observed during the above polymerization. First, these swollen and fluid four-component systems have flexible and fluctuating interfaces[23,26], much more labile than the rigid layers of concentrated ($C_s \simeq 0.7$) and viscous binary or one-phase component(s). In the former case, the layers are only flat at scales smaller than the persistence length of the film and can easily undergo deformations. In addition, highly curved local defects might be present as reported for similar birefringent microemulsions[23,26,27]. Repulsive undulation forces of entropic origin were shown to be at the origin of the stability of hyperswollen lamellar phases[21,22].

The second important factor involved in the structural modification comes from the monomer itself. Thorough studies of acrylamide microemulsions by light scattering, viscometry and conductivity have revealed the strong influence of this monomer on the interfacial properties of the systems[28–30]. In particular, a notable extension of the one-phase domain in the phase diagram was observed, indicating that AM acted as a co-surfactant and was partially located between the surfactant molecules, thus increasing the flexibility of the film. The surface-active properties of this monomer were also confirmed by surface tension experiments[31]. In the case of bicontinuous microemulsions, the amount of AM located at the water/oil interface was estimated to be of the order of 30%[11].

The existence of fluctuating membranes containing a significant part of the monomer permits one to understand the results. There is no need to invoke the entropy loss during polymerization and the energy of confinement of a high-molecular-weight polymer in a restricted layer thickness of 80 Å. Indeed, the simple effect of polymerization on the interfacial energy of the systems seems to be the key parameter. As soon as the polymerization starts, the monomer consumption from the layers induces a change in the film curvature energy, which destabilizes the system and gives rise to a shift in the phase diagram. A two-phase equilibrium forms between a lamellar phase with zero curvature and an upper isotropic phase with a spontaneous curvature, which can be either bicontinuous or of globular type. Both phases contain all of the components, which shows that the monomer is not the only component expelled from the lamellar phase.

The diagrams of *Figure 6* show an important feature of the process, namely the coexistence of one latex phase with two reservoir phases of lamellar and microemulsion-like types. One can speculate that the polymerization starts in the upper microemulsion phase in a similar way to that described elsewhere[12,28]. Gravity forces due to the very large difference in density between polymer ($\simeq 1.39$) and monomer (1.12) would cause the newly formed polymer particles to settle at the bottom of the flask. As polymerization proceeds, the volume of the lower latex phase grows at the expense of that of the reservoir lamellar phase. The composition and volume of the upper reservoir microemulsion is maintained constant at the equilibrium (saturation) level by diffusion of components from the lamellar phase, whose volume and periodicity shrink with time. After the total disappearance of the lamellar phase (step (e) in *Figure 6*), the composition of the upper phase is no longer maintained at the saturation level; the phase becomes turbid and unstable, until complete polymerization has taken place. Finally, when all of the monomer has reacted, an optically transparent isotropic and stable latex is produced with the characteristics described in the 'Experimental' section. It is likely that a similar mechanism controls the polymerization of AM in bicontinuous microemulsions; the latter are also characterized by the appearance of turbidity and viscosity increase during polymerization[10,12]. In both cases, the polymerization rate is very high and the molecular weight of the polymer is of the order of 5×10^6.

It should be noted that this mechanism is very reminiscent of that reported for conventional emulsion polymerization, where a monomer reservoir phase exists in the form of polydisperse macroscopic droplets[32]. The original feature of acrylamide polymerization in the lamellar phase lies in the fact that, all through the polymerization reaction, the monomer is located in the aqueous phase of a microemulsion. This is the reason for the small particle size produced by such a process.

ACKNOWLEDGEMENTS

The authors wish to thank Drs P. Pincus and G. Porte for stimulating discussions. They are also grateful to A. Schierer and S. Graff for their technical assistance.

REFERENCES

1 Barrall, E. M. and Johnson, J. F. *J. Macromol. Sci., Rev. Macromol. Chem. (C)* 1979, **17**(1), 137
2 Blumstein, A. (Ed.), 'Liquid Crystalline Order in Polymers', Academic Press, New York, 1978
3 Blumstein, A., Clough, S. B., Patel, L., Blumstein, R. B. and Hsu, E. C. *Macromolecules* 1976, **9**, 243
4 Finkelmann, H., Happ, M., Portugal, M. and Ringsdorf, H. *Makromol. Chem.* 1978, **179**, 2541
5 Finkelmann, H., Koldehoff, J. and Ringsdorf, H. *Angew. Chem.* 1978, **90**, 992
6 Herz, J., Reiss-Husson, F., Rempp, P. and Luzatti, V. *J. Polym. Sci.* 1963, **4**, 1275
7 Friberg, S. E., Thundatil, R. and Stoffer, J. O. *Science* 1979, **205**, 607
8 Thundatil, R., Stoffer, J. O. and Friberg, S. E. *J. Polym. Sci., Polym. Chem. Edn.* 1980, **18**, 2629
9 Tsutui, T. and Tanaka, T. *J. Polym. Sci., Polym. Lett. Edn.* 1977, **15**, 475
10 Holtzscherer, C., Durand, J. P. and Candau, F. *Colloid Polym. Sci.* 1987, **265**, 1067
11 Holtzscherer, C. and Candau, F. *Colloids Surf.* 1988, **29**, 411
12 Holtzscherer, C. and Candau, F. *J. Colloid Interface Sci.* 1988, **125**, 97

13 See, for example, Bellocq, A. M., Biais, J., Bothorel, P., Clin, B., Fourche, G., Lalanne, P., Lemaire, B., Lemanceau, B. and Roux, D. *Adv. Colloid Interface Sci.* 1984, **20**, 167
14 Guinier, A. and Fournet, G. in 'Small-Angle Scattering of X-Rays', Wiley, New York, 1955
15 Baro, R. and Luzzati, V. *J. Phys. Rad.* 1961, **22**, 186A
16 François, J., Sarazin, D., Schwartz, T. and Weill, G. *Polymer* 1979, **20**, 969
17 Benton, W. J., Fort, T., Jr. and Miller, C. A. *Soc. Petrol. Eng. Reprint* 1978, 7579
18 Candau, F., Ballet, F., Debeauvais, F. and Wittmann, J. C. *J. Colloid Interface Sci.* 1982, **87**, 356
19 Hirsch, E., Wittmann, J. C. and Candau, F. *J. Disp. Sci. Technol.* 1982, **3**, 351
20 Larché, F. C., Appel, J., Porte, G., Bassereau, P. and Marignan, J. *Phys. Rev. Lett.* 1986, **56**, 1700
21 Porte, G., Bassereau, P., Marignan, J. and May, R., in 'Physics of Amphilic Layers', (Eds J. Meunier, D. Langevin and N. Boccara), Springer-Verlag, Berlin, 1987, p. 145
22 Roux, D. and Safinya, C., in ref. 21, p. 138
23 di Meglio, J. M., in ref. 21, p. 153
24 Candau, F. and Holtzscherer, C. *J. Chim. Phys.* 1985, **82**, 691
25 Anderson, D. M. and Ström, P., in 'Polymer Association Structures, Microemulsions and Liquid Crystals', (Ed. M. El Nokaly), ACS Symp. Ser., Washington DC, 1989, Ch. 13, p. 204
26 di Meglio, J. M., Dvolaitzky, M. and Taupin, C. *J. Phys. Chem.* 1985, **89**, 871
27 di Meglio, J. M., Dvolaitzky, M., Ober, R. and Taupin, C. *J. Phys. Lett.* 1983, **44**, L229
28 Candau, F., Leong, Y. S., Pouyet, G. and Candau, S. J. *J. Colloid Interface Sci.* 1984, **101**, 167
29 Candau, F., in ref. 25, Ch. 4, p. 47
30 Carver, M. T., Hirsch, E., Wittmann, J. C., Fitch, R. M. and Candau, F. *J. Phys. Chem.* 1989, **93**, 4867
31 Pichot, C., Graillat, C. and Revillon, A., Proc. XVII Congr. AFTPV, Nice, 1987, p. 270
32 Smith, W. V. and Ewart, R. V. *J. Chem. Phys.* 1984, **16**, 592